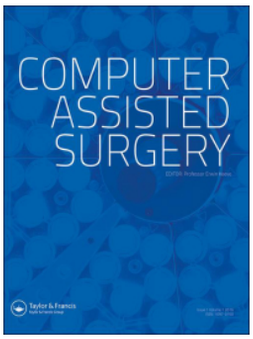

Journal of Image Guided Surgery

ISSN: 1078-7844 (Print) (Online) Journal homepage: informahealthcare.com/journals/icsu19

Mathematical Determination of the Tibial Insertion of the Patellar Tendon Using Computed Tomography Images

Guillaume Champleboux, Remi Julliard, Philippe Cinquin & Line Gaborit

To cite this article: Guillaume Champleboux, Remi Julliard, Philippe Cinquin & Line Gaborit (1995) Mathematical Determination of the Tibial Insertion of the Patellar Tendon Using Computed Tomography Images, Journal of Image Guided Surgery, 1:4, 226-236, DOI: 10.3109/10929089509106328

To link to this article: https://doi.org/10.3109/10929089509106328

Published online: 06 Jan 2010.

Submit your article to this journal

Article views: 376

View related articles

Full Terms & Conditions of access and use can be found at
https://informahealthcare.com/action/journalInformation?journalCode=icsu21

Laboratory Investigation

Mathematical Determination of the Tibial Insertion of the Patellar Tendon Using Computed Tomography Images

Guillaume Champleboux, Ph.D., Remi Julliard, M.D.,
Philippe Cinquin, Ph.D., M.D., and Line Gaborit
TIMC-IAB, Faculté de Medecine de Grenoble, La Tronche, France (G.C., P.C., L.G.); Clinique mutualiste-Rocheplane, Grenoble, France (R.J.)

ABSTRACT Misalignment of the extensor apparatus is an essential factor in impairment of the patellar-femoral joint. This may be partly or entirely responsible for patellar dislocation or lateral patellar-femoral arthrosis. One surgical method to correct the pathology is medial transposition of the patellar ligament on the tibial tuberosity (anteriorly or posteriorly, distally or ventrally). These interventions correct misalignment of the extensor apparatus relative to statistical norms. We propose a mathematical method based on the use of computed tomography (CT) images to determine the ideal tibial insertion for the patellar tendon. This method is based on biomechanical modeling and the use of equipressure criteria. It is the first step in allowing the use of mathematics to model correctly tibial insertion of the patellar ligament, an entirely new development. This is important because it will allow surgeons greater accuracy in distal correction of extensor apparatus misalignments. *J Image Guid Surg* **1:226–236 (1995)** ©1996 Wiley-Liss, Inc.

Key words: **tibia, patella, patellar tendon, transposition, biomechanic**

INTRODUCTION

Patellar instability and distal femoropatellar arthrosis have several etiologies. One of them is extensor apparatus misalignment. Let us consider that the vector representing the quadriceps and the pulley made by the femoral trochlea are both fixed. The misalignment of the extensor apparatus presents a position defect on the anterior tibial tuberosity (ATT) at the tibial insertion of the patellar tendon. Notably, for a given patellar tendon, the tibial insertion site can either be too external or too proximal. It is easy to use the patellar index of Caton and Deschamps[4] to normalize the position of the ATT along the proximal/distal direction. It is more often debated and more difficult to determine the length of the inner transposition of an obviously excessively external ATT.

Currently, two methods exist to measure misalignment in the coronal plane: Anglo-American surgeons use the quadriceps angle[11] (i.e., the angle made by the quadriceps tendon with the patellar tendon), whereas French physicians use the TAGT measure [tuberosité antérieure-gorge de la trochlée (ATTG), which in English stands for anterior tuberosity-trochlear groove].[2] This measure is the distance in millimeters between two parallel vertical lines projected on the coronal plane of the ATT and perpendicular to the tangent joining both posterior femoral condyles. One vertical line intersects the top of the tibial tuberosity, and the other intersects the proximal part of the trochlear groove (Figs. 1, 2). It is still debated whether the ATTG must be measured with the knee in full ex-

Received original September 22, 1995; accepted January 31, 1996.

Address correspondence/reprint requests to Guillaume Champleboux, TIMC-IAB, Faculté de Medecine de Grenoble, 38700 La Tronche, France.

©1996 Wiley-Liss, Inc.

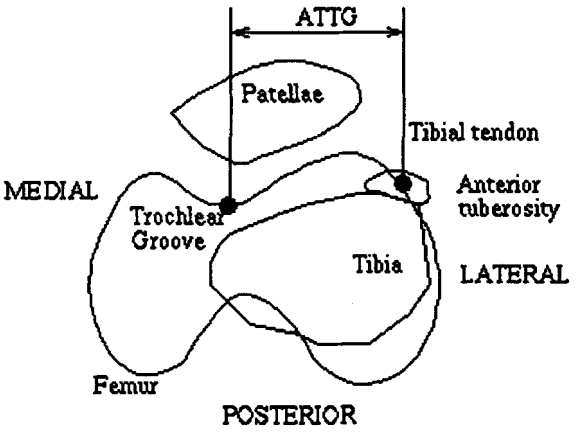

Fig. 1. Definition of the ATTG.

tension or at a 15° angle of flexion. We measure the ATTG with the knee in full extension to enhance reproducibility. It is assumed that an inner transposition of a ATT that is too external tends to "normalize" the ATTG to a value between 10 to 15 mm (in full extension). In this paper, a different mathematical approach to this problem is offered, based on biomechanical hypotheses described in the next section.

In this model, practical considerations and simplicity dictate that 1) we consider geometric features with the knee in full extension and 2) we deal only with mathematical determination of the inside simple anterior tibial tuberosity transposition (ATTT), without Maquet or anti-Maquet effects and without proximal or distal displacement (associated parasites). In later sections, we describe mathematical modeling of the hypotheses, give the data obtained using computed tomography (CT) images for this model, give the mathematical calculus of the transposition, and discuss our results.

BIOMECHANICAL STUDY

Notation

In the general case, let the force created by the quadriceps be F_q, let the force created by the patellar tendon be F_t, and let the knee flexion angle be at a defined position θ. R is the sum of those two forces (see Fig. 2):

$$R = F_t + F_q \tag{1}$$

The study of the spatial direction and position of R in a known reference coordinate system will give a numerical indication for the misalignment and helps to quantify the surgical maneuver in function of the effect desired. The resultant R exerts itself on the contact sites between the two trochlear cheeks and the patella. This area is divided into S_i (the contact area on the internal trochlear cheek) and S_e (the contact area on the external trochlear cheek). Let P be the plane perpendicular to the proximal part of both S_i and S_e. When the knee is in full extension, P is the horizontal plane (see Fig. 3). R_p is the projection of R on the plane P, and F_i and F_e are, respectively, the projections of R_p on the lines perpendicular to the internal and external trochlear cheeks.

Biomechanical Data

This section presents the results of research done by other authors. These results will be useful later as indications for the present model.

1. Huberti et al.[9] showed that the intensity of F_t and F_q are not always equal. In fact,

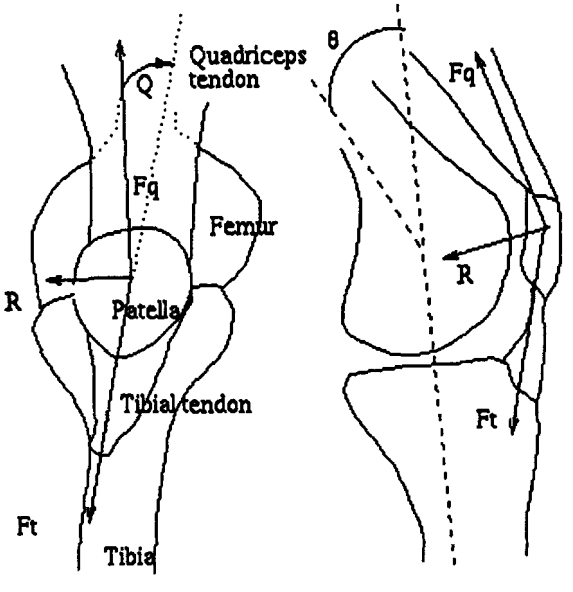

Fig. 2. Spatial position of F_q, F_t and R.

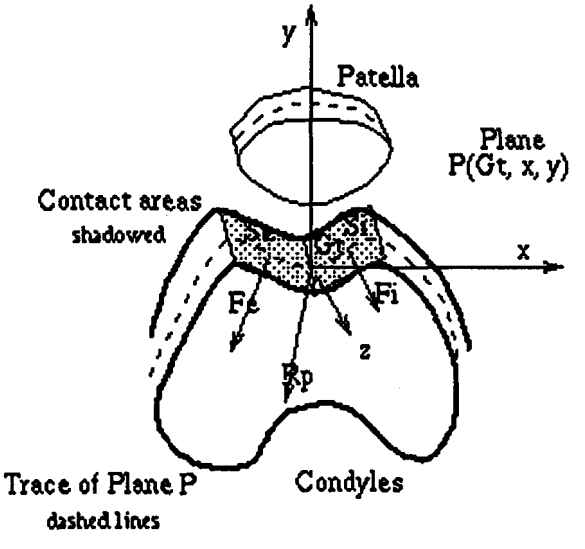

Fig. 3. Geometric features and notations.

$$\|F_t\| = k(\theta)\cdot\|F_q\| \qquad (2)$$

with the values (k,θ):(1,0°) (1.27,30°) (0.91,60°) (0.70,90°).

2. The patellar-femoral contact pressure is highest between 60° and 90° of flexion (see Huberti and Hayes[8]).

3. Chondromalacial lesions occur most frequently in regions corresponding to contact areas at between 40° and 80° of flexion (see Seedhom et al.[20]).

4. Fujikawa et al.[6] studied the pattern of contact and the congruence of the patellar-femoral joint. Their work shows that 1) the lateral side has the largest contact area and 2) the patellar facet angle and the trochlear femoral angle show different values at contact sites for different angles of flexion. Therefore, S_i and S_e depend on θ.

5. Patellar dislocation occurs at the beginning of knee flexion.

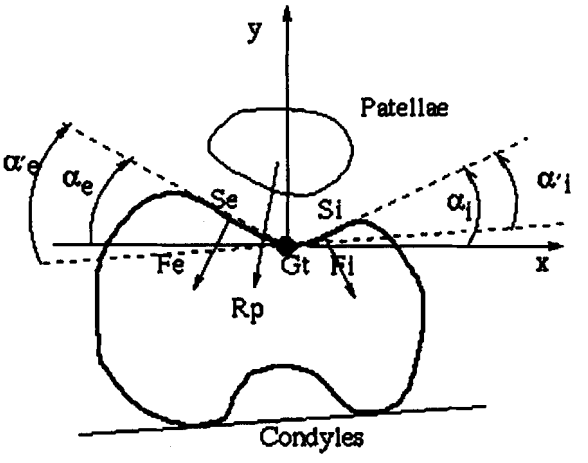

Fig. 4. Further geometric features and notations.

Practical Constraints

CT data are acquired with the subject's knee in full extension. This is significant because the angle of flexion is near 0° and all S_i, S_e, α_i, α_e, F_i, F_g vary according to θ. Although Garg and Walker[7] have made a three-dimensional (3-D) model of knee motion using cadavers, a 3-D dynamic study has not been made because it entails increasing the time of patient examinations, thus increasing X-ray exposure, cost, time, and services from of personnel and equipment. Although in the future a 3-D dynamic model will have to be developed for the patellar-femoral joint, for the present we can use the data already available. Thus we consider the biomechanical configuration as constant. This hypothesis is less restrictive than it appears to be, because patellar dislocations occur at the beginning of flexion ($\theta < 10°$), and the data were acquired with the knee in full extension ($\theta \cong 0°$).

Let us define a reference coordinate system in which the x axis is the lateral-medial axis and the y axis is the sagittal axis. The origin G_t is the intersection of the two trochlear cheeks in the plane P. α_i is the angle between the x axis and the trace of the internal side of the trochlea in plane P, α_e is the angle between the x axis and the trace of the external side of the trochlear in plane P. The classical notation considers α'_e and α'_i as the angles between the line representing the coronal plane tangent to both femoral condyles and the lines representing the external or internal sides of the trochlea, respectively (see Fig. 4).

Biomechanical Hypotheses

Let ϕ be the angle between x and R_p, and ϕ_i and ϕ_e the angles between x and, respectively, F_i and F_e (Fig. 5). The quadriceps by itself dynamically stabilizes the patella if the R_p force is situated in the security triangle delimited by the two perpendiculars to the two trochlear cheeks.[12,13,17] Depending on which CT images are used, it is necessary to distinguish between right and left knees. This dynamic stabilization is ideal if the F_e and F_i forces (which are the projections of R_p on the lines perpendicular to the trochlear cheeks) are proportional to the external S_e and internal S_i surfaces of these trochlear cheeks. Therefore, ideally, the two facets of a stable and correctly balanced patella exert the same pressure on the two corresponding cheeks of the trochlea (see Fig. 5). It is not possible to measure exactly the values S_i and S_e using CT data, which is why the assumption is made that the ratio $\frac{S_i}{S_e} = r_s$ is equal to $\frac{L_i}{L_e}$. L_i and L_e represent S_i and S_e in the plane P (for experimental results, see Maquet[18] and Townsend et al.[21]). The values L_i and L_e are easily identified on a determined CT slice.

We can summarize the two hypotheses as follows. Hypothesis 1 (hypothesis of minimal constraint): R_p is in the security triangle; this implies:

$$\phi_e \geq \phi \geq \phi_i \text{ (right)}$$
$$\phi_e \leq \phi \leq \phi_i \text{ (left)} \qquad (3)$$

Hypothesis 2 (hypothesis of ideal constraint): R_p makes an angle ϕ_{ideal} with the x axis such that

$$\frac{F_i}{L_i} = \frac{F_e}{L_e} \qquad (4)$$

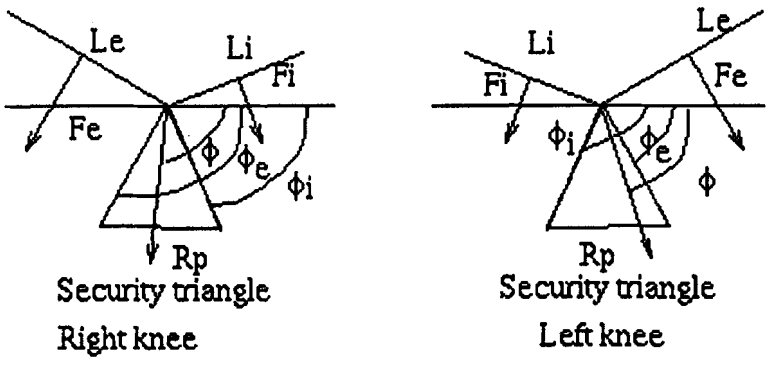

Fig. 5. Geometric features for hypothesis 1.

Surgical Constraint

Lateral patellar dislocation or lateral patellar-femoral arthrosis can be corrected by a patellar tendon transposition on the inner side of the tibial tuberosity. To determine the amplitude of this transposition, a mathematical model of this problem is proposed using the two hypotheses given above. Nevertheless, we offer additional hypotheses that express surgical constraint and experimental knowledge. If one considers that one of the two points that gives the direction of F_t is the tibial insertion of the tendon on the tibial tuberosity, transposing this point implies modifying F_t. We choose 1) to impose no proximal or distal displacement of the patellar tendon, so that the z coordinate of F_t is constant (When the patella is too high, the surgeon lowers it; it is a distal transposition of the ATT.) and 2) to have no Maquet or anti-Maquet effect; this implies that the y coordinate of F_t is constant (when patellar-femoral arthrosis is present, the surgeon can place the ATT anteriorly). The study is done in the case of a simple transposition along the x axis with the knee in full extension.

MATHEMATICAL MODEL

Notation

The reference coordinate system is defined by: the x axis (medial/lateral), the y axis (anterior/posterior), the z axis (proximal/distal axis), and the origin G_t. F_q is $(F_{q_x}, F_{q_y}, F_{q_z})$. F_t is $(F_{t_x}, F_{t_y}, F_{t_z})$. F_t^* $(F_{t_x}^*, F_{t_y}^*, F_{t_z}^*)$ is the force created by the patellar tendon after transposition (minimal case: $F_t^* = F_t^{minimal}$, ideal case: $F_t^* = F_t^{ideal}$).

R is (R_x, R_y, R_z); R^* (R_x^*, R_y^*, R_z^*) is the result of F_q and F_t^*. R_p $(R_x, R_y, 0)$ is the projection of R in plane P.

F_i $(F_{i_x}, F_{i_y}, 0)$ and F_e $(F_{e_x}, F_{e_y}, 0)$ are the orthogonal R_p projection on the internal and external trochlear cheeks in P. R_p^* $(R_x^*, R_y^*, 0)$ is the projection of R^* in plane P. R_{pideal} is the projection of R_{ideal}. $R_{minimal}$ is the projection of $R_{minimal}$.

Direction of $R_p^* = R_{pminimal}$ According to Hypothesis 1

Wherever the R_p^* force is applied, we consider the angle formed by the direction of the force relative to the x axis. R_p^* must be in the security triangle. In the simplest case, this angle corresponds to the angle between the x axis and F_e and is denoted $\phi_{minimal}$ (see Fig. 6). For the right knee, $\phi_{minimal} = -\pi/2 - \alpha_e$. For the left knee, $\phi_{minimal} = -\pi/2 + \alpha_e$.

Direction of $R_p^* = R_{pideal}$ According to Hypothesis 2

For the right knee, because $\frac{L_i}{L_e} = \frac{S_i}{S_e}$ one has a direct relationship: ϕ_{ideal}, α_e, α_i, L_i, and L_e.

$$\tan(\phi_{ideal}) = \frac{L_i \cdot \cos(\alpha_i) + L_e \cdot \cos(\alpha_e)}{\epsilon \cdot L_i \cdot \sin(\alpha_i) - \epsilon \cdot L_e \cdot \sin(\alpha_e)} \quad (5)$$

For the right knee $\epsilon = 1$; for the left knee $\epsilon = -1$.

Mathematical Relation Involving Force Components

Transposition according to the surgical constraint is possible only along the x axis. Let ϕ^* be $\phi_{minimal}$ or ϕ_{ideal}, and we have the relation:

$$F_{t_x}^* + F_{q_x} = R_x^* = R^* \cdot \cos(\phi^*)$$
$$F_{t_y} + F_{q_y} = R_y^* = R^* \cdot \sin(\phi^*)$$

which gives:

$$F_{t_z}^* = -F_{q_x} + \cot g\ (\phi^*) \cdot (F_{t_y} + F_{q_y})$$

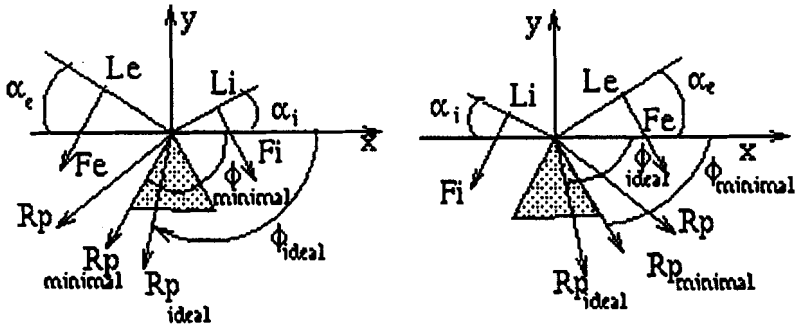

Fig. 6. Geometric features for the right and left knees.

ACQUIRING NUMERICAL DATA USING CT IMAGES

Data Available with Computed Tomography

The data obtainable are a set of CT slices acquired with the patient lying on the scanner table with the knee in full extension (see Figs. 11, 12). In the reference coordinate system of the scanner, we can extract from these slices (see Fig. 7) 1) the coordinates of the tibial insertion of the patellar tendon. (mean of three slices; see Figs. 12, 13); this point is denoted T_a (T_{a_x}, T_{a_y}, T_{a_z}); 2) information about the contact areas between trochlea and patella, i.e, the length of the external and internal trochlear cheeks L_i, L_e, and the angles these cheeks make with the x axis, α_i, α_e. The coordinates of the intersection point of these two cheeks are denoted G_t (G_{t_x}, G_{t_y}, G_{t_z}); (see Fig. 15); and 3) a set of N_s slices (N_s ranges from 8 to 11) containing information about the quadriceps. It is possible to determine the surface of the quadriceps and the gravity center Q_{gi} (Q_{gi_x}, Q_{gi_y}, Q_{gi_z}) of the quadriceps on each surface (see Fig. 16).

The reference coordinate system of the scanner, denoted R_t, is the same as that defined above under Notation, with only a translation between the origin of the scanner and the point G_t. This small difference does not affect the calculus because vectorial coordinates are used.

Features of F_t

The direction of F_t is defined by two points. One is T_a (T_{a_x}, T_{a_y}, T_{a_z}). For the second, we successively opted 1) for the bottom point of the trochlear groove, although this point is notadequately representative from a biomechanical standpoint; 2) for the patella center of gravity, although Merchant et al.[19] showed that the patella moves significantly depending of the contraction or relaxation of the quadriceps and that the measure is not repeatable; and 3) finally for the fictive point defined as the intersection of the two medians of the trochlear cheeks (see Figs. 8, 14). This point is denoted S_t. (See Fig. 8)

The coordinates of S_t are (S_{t_x}, S_{t_y}, S_{t_z}) with:

$$S_{t_x} = G_{t_x} + \frac{\epsilon \cdot L_i \cdot \sin(\alpha_e) - \epsilon \cdot L_e \cdot \sin(\alpha_i)}{2 \cdot (\cos(\alpha_i) \cdot \sin(\alpha_e) + \cos(\alpha_e) \cdot \sin(\alpha_i))}$$

$$S_{t_y} = G_{t_y} + \frac{\epsilon \cdot L_i \cdot \cos(\alpha_e) - \epsilon \cdot L_e \cdot \cos(\alpha_i)}{2 \cdot (\cos(\alpha_i) \cdot \sin(\alpha_e) + \cos(\alpha_e) \cdot \sin(\alpha_i))}$$

$$S_{t_z} = G_{t_z}$$

($\epsilon = 1$ for the right knee, and -1 for the left knee). Finally, F_t is colinear to the vector $\overrightarrow{S_t T_a}$. It exists $\lambda \in R_+$ such that

$$F_t = \lambda \cdot \overrightarrow{S_t T_a} \tag{7}$$

Features of F_g

We assume that the direction of F_g is given by the point S_t and the quadriceps center of gravity (QGC) Q_g (Q_{g_x}, Q_{g_y}, Q_{g_z}). Let us call D the domain of the quadriceps; we have:

$$Q_{g_{var}} = \frac{\int_D var \cdot dx \cdot dy \cdot dz}{\int_D dx \cdot dy \cdot dz} \tag{8}$$

(*var* is either x, y, or z). To make an evaluation of the center of the QGC, we take into account each scanner slice where the quadriceps appears. On each slice referenced by $i = 1 \ldots n$, the quadriceps is detected on an area A_i associated with a height called Z_i and a thickness dh. We call Q_{g_i} ($Q_{g_{ix}}$, $Q_{g_{iy}}$, $Q_{g_{iz}}$) the center of gravity of the part of the quadriceps appearing in the slice i. Let S_{slice_i} be $S_{slice_i} = \int_{A_i} dx \cdot dy$. The ap-

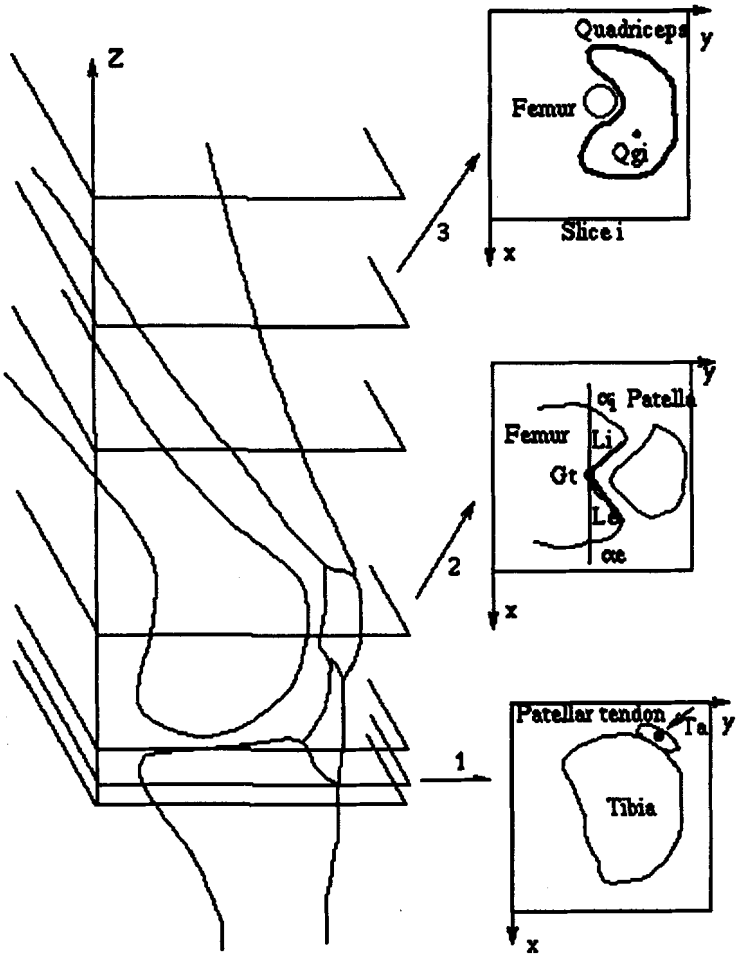

Fig. 7. Description of the CT slices.

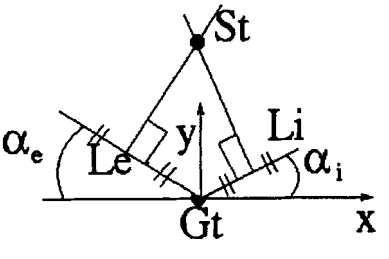

Fig. 8. Determination of the S_t point.

proximated coordinates of Q_g in R_o are given by:

$$Q_{g_{var}} = \frac{\sum_{i=1}^{n} Q_{gi_{var}} \cdot S_{slice_i}}{\sum_{i=1}^{n} S_{slice_i}} \quad (9)$$

(*var* is either *x*, *y*, or *z*). Finally F_q is colinear to the vector $\overrightarrow{S_t Q_g}$. It exists $\lambda' \in R_+$ such that

$$F_q = \lambda' \cdot \overrightarrow{S_t Q_g} \quad (10)$$

Let f^* be

$$f^* = \frac{\left\| \overrightarrow{S_t T_s^*} \right\|}{\left\| \overrightarrow{S Q_g} \right\|} \quad then \quad \frac{\gamma'}{\lambda} = \frac{f^*}{k(\theta)} \quad (11)$$

with $k(\theta) = 1$, because θ is near 0°.

VALUE OF THE PATELLAE TENDON TRANSPOSITION

Determination of the New Tibial Insertion

Let T_a^* be the new point of insertion with the coordinates $(T_{a_x}^*, T_{a_y}, T_{a_z})$. By using equations 6, 7, 10, and 11, the final formula becomes:

$$T_{a_x}^* - S_{t_x} = -f^* \cdot (Q_{g_z} - S_{t_z}) + \cot g(\phi^*) \cdot (T_{a_y} - S_{t_y} + f^* \cdot (Q_{g_y} - S_{t_y})) \quad (12)$$

The difference Δx such that:

$$\Delta x = T_{a_x}^* - T_{a_x} = F_{t_x}^* - F_{t_x} \quad (13)$$

indicates the amplitude of possible transposition on the inner side of the tibial tuberosity.

Uncertainties

To deal with uncertainties on scanner data measurements, we differentiated Δ_x relative to L_i, L_e, α_i, α_e, S_{t_x}, S_{t_y}, Q_{g_x}, Q_{g_y}. The error is estimated to about 1 mm for L_i, L_e, S_{t_x}, S_{t_y}; 3 mm for Q_{g_x}, Q_{g_y}; and about 1° for α_i, α_e.

To achieve Q_{g_x}, Q_{g_y}, Q_{g_z}, we use a segmentation interface, which allows each area A_i to be determined for each CT slice *i*. The quadriceps is manually segmented, and some errors can occur. A repetitive test for the segmentation gave good results, because the coordinates of Q_g vary by less than 3 mm.

Another origin of errors is the state of the quadriceps during the scan; i.e., is the quadriceps relaxed or contracted? The data were acquired from five patients with quadriceps contracted (Q_{g_c}) and then relaxed (Q_{g_r}). The result is that the distance between Q_{g_c} and Q_{g_r} is less than 3 mm, so the state of the quadriceps has a negligible influence in determining Q_g (see Fig. 10).

RESULTS

Results from a 3D Representation

Figure 9 explains Figure 10, which shows the 3-D position of the data used. Figure 9 was obtained with the AVS software. In Figure 10, data for both contracted and relaxed quadriceps are presented. We have represented the line (MS line) that fits the set of intermediate gravity centers to the mean square criterion.

This representation shows that 1) a line exists that joins the intermediate gravity centers with very good approximation, 2) the center of gravity Q_g is really near the middle of the MS line (the distance between Q_g, and *MS* is less than 3 mm), and 3) the direction of *MS* passes beneath the trochlear cheeks. In fact, the quadriceps is made of four heads [vastus intermedius (VI), rectus femoris (RF), vastus medialis

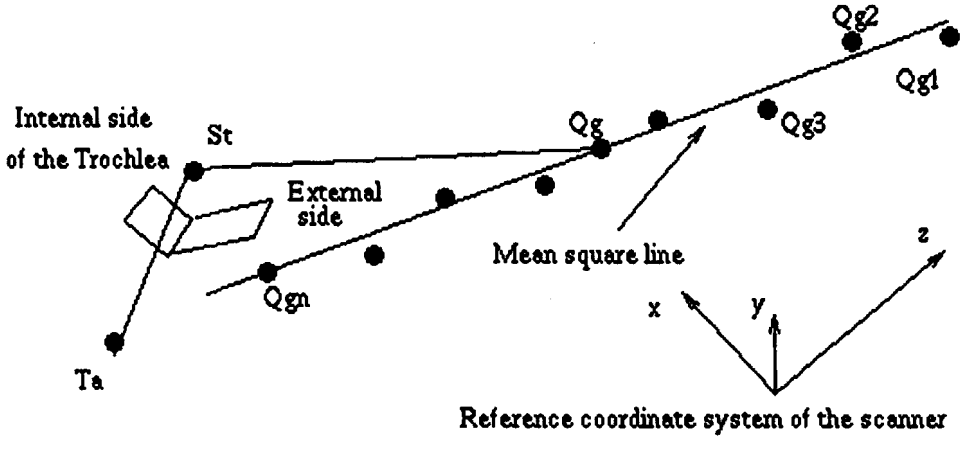

Fig. 9. Line passing by the center of gravity of each slice.

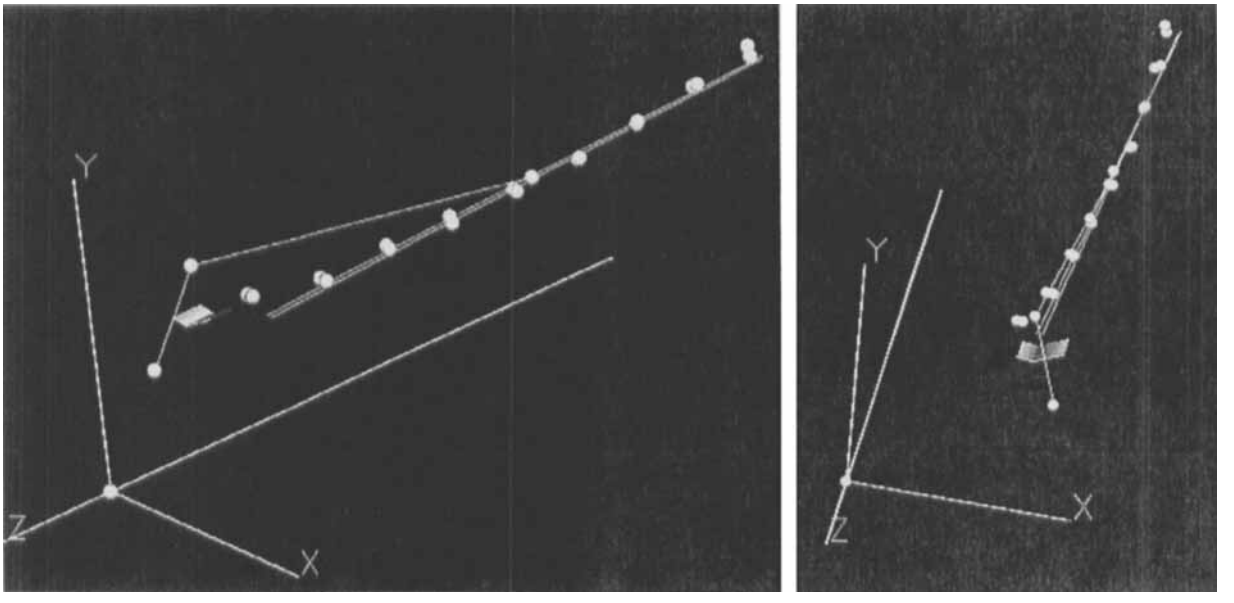

Fig. 10. Line passing by the gravity center of each slice. Data for both contracted and relaxed quadriceps are represented.

(VM), and vastus lateralis (VL)]. Every head has fibers with individual directions.[1,15,16] The final direction is a combination of the four directions. We assume that this final direction of F_q is given by the line passing by S_t and Q_g; this seems to be the most useful compromise. Also, 4) the direction of F_t (given by S_t and T_a) and F_q effectively shows the possibility of lateral subluxation.

Numerical Results

Table 1 contains 1) the patient number in column Pat; 2) the concerned side (L for left, R for right) in column S; 3) the value of the Q angle (in degrees) in column Q angle; 4) the value of the ATTG (in millimeters) in column ATTG; 5) in the ST column, Y means that R_p is in the security triangle, and N means that R_p is not in the security triangle (in the latter case, there is a possibility of lateral subluxation); 6) the value (in millimeters) of the transposition in the case of hypothesis 1 in column $\Delta x_{minimal}$); 7) the value (in millimeters) of the transposition in the case of hypothesis 2 in column Δx_{ideal}; 8) the error (in millimeters) made on the calculus in column Error; 9) the

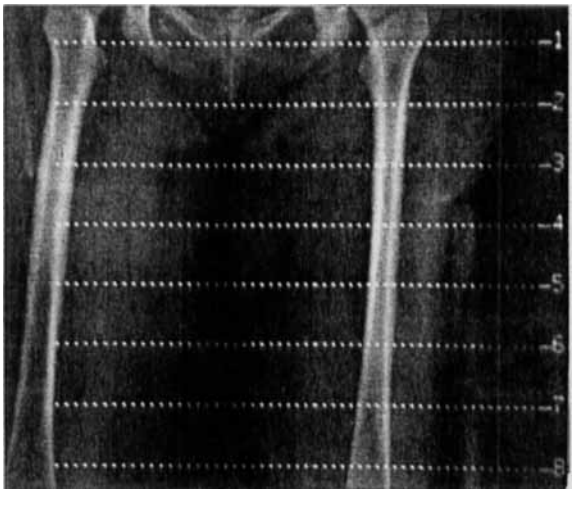

Fig. 11. CT acquisition: 1) the quadriceps.

Fig. 12. CT acquisition: 2) the T_a point.

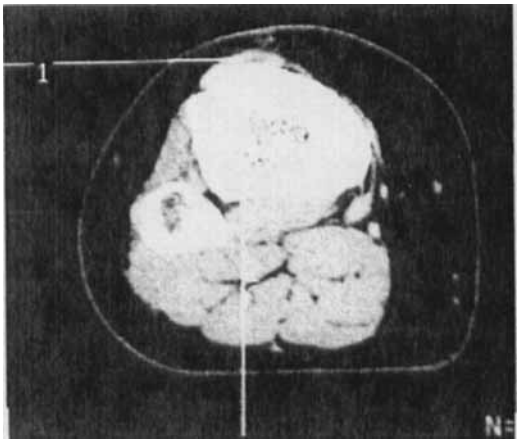

Fig. 13. Determination of T_a.

value (in degrees) of the Q angle calculated for $\phi_{minimal}$ in column $Q_{minimal}$; 10) the value (in degrees) of the Q angle calculated for ϕ_{ideal} in column Q_{ideal}; 11) the value (in millimeters) of the ATTG calculated for $\phi_{minimal}$ in column $ATTG_{minimal}$; and 12) the value (in millimeters) of the ATTG calculated for ϕ_{ideal} in column $ATTG_{ideal}$.

A classical norm for the ATTG is 10–15 millimeters and 15° for the Q angle.[10] In most the cases (patients 13 and 15 are exceptions), the projection of the R_p force is out of the security triangle. These results are in accordance with the pathological phenomenon. The computed inner transposition (positive for the right knee and negative for the left knee) is useful in most cases, as shown in column Δx_{min}, and in most cases is too high, as shown in column Δx_{ideal}.

In fact, in the minimal case, the inner transposition tends to normalize both the Q angle and the ATTG values. In the ideal case, the Q angle is near

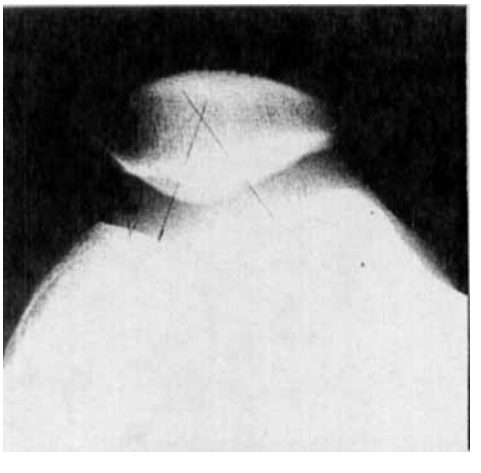

Fig. 14. Determination of S_t.

Fig. 15. Determination of L_i, L_e, α_i, α_e, G_t.

0° and the ATTG is near 0 mm. The results of the ideal case correspond to the state reached by a normal patellar-femoral joint near 90° of flexion.

It seems that the ideal case introduces a very strong constraint. The hypothesis of equipressure is very important when the contact pressure is maximal (between 60° and 90° of flexion). At this stage, the configuration is completely different from that when the knee is in full extension, because there is an abduction of the knee of about 20°.[3] Experiments have been inconclusive regarding ideal constraints.

Movement of the patellar-femoral joint will have to be dealt with in the future using a 3D model. The hypothesis of equipressure (ideal constraint) should be studied between 60° and 90° of flexion where chondromalacia occurs most frequently. The

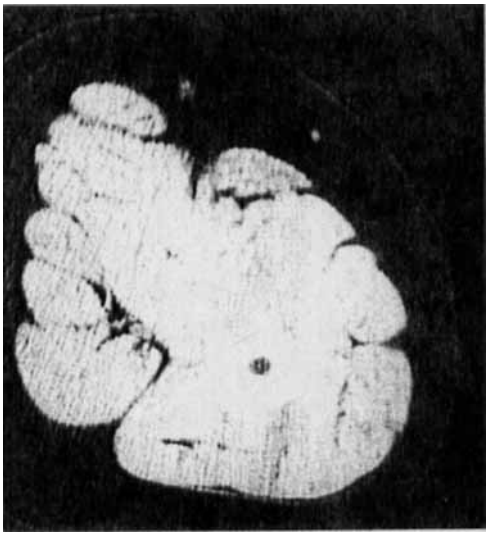

Fig. 16. A slice for quadriceps segmentation.

minimal constraint is well adapted in our configuration (knee near 0° of flexion) because it provides a good model for correction of subluxation, which occurs at the beginning of flexion.

Future Work

Determination of the center of gravity of the quadriceps is a very delicate part of our method. Even with software adapted to segment the quadriceps on every CT slice and to calculate the area, the segmentation time is too great. Moreover, reducing manipulation by radiology personnel reduces costs. To simplify the procedure, it is possible to acquire only three CT slices: 1) one passing through the middle position of the quadriceps, 2) one passing through the mean attachment point of the tibial tendon on the tibial tuberosity, and 3) one passing through the contact area between the patella and the femur.

With these three slices, it is possible to extract all the data needed. Tests have been done to evaluate the error generated by this simplification. The only difference concerns QGC determination. As was explained above under Results From a 3D Representation, Q_g is quite near the MS line. Taking the middle of the segment $Q_{g1}Q_{gNs}$ as Q_g generates an error smaller than 2 mm on Δx. For this reason, the QGC of the slice passing through the middle of the quadriceps gives a good estimation of the global QGC at present determined by N_s intermediate slices.

It would be interesting and complementary to work on data acquired with the knee at 90° of flexion using the same model, especially when the equipressure constraint is applied. In using the simplification described above, only six slices for each patient are needed, which is a good compromise regarding X-ray dose, cost, and time. The main interest will lie in comparing Δx_{ideal} with the knee at 90° of flexion and $\Delta x_{minimal}$ with the knee at 0° of flexion.

CONCLUSIONS

A new model for the patellar-femoral joint has been developed and can be used as a starting point for other accurate models. By using CT data, it is possible to compute the ATTT with respect to two criteria, which depend on a biomechanical model and biomechanical hypotheses. According to the criteria of minimal constraint (correction of subluxation), the computed value of the transposition fits well with the concept of the ATTG and the common values (5–15 mm) applied during interventions. The criteria of ideal constraint (equipressure of the two trochlear cheeks) gives excessive values for the inner transposition (15–25 mm). In fact, the CT data acquired with the knee fully extended should not be used with this criterion. In the future, it will be necessary to add CT data with the knee at 90° of flexion and to observe whether the two criteria (minimal at 0° and ideal at 90°) are redundant. In any case, these preliminary results are a link between a diagnosis of patellar dislocation and surgical interventions that entail an inner transposition of the ATT. Theoretical research and clinical work have to be continued for model and laboratory validations.

Table 1. Numerical Results Obtained from Clinical Data

Pat.	S.	Q angle	ATTG	ST	$\Delta\chi min$	$\Delta\chi ideal$	error	*Q min*	*Q ideal*	*ATTG min*	*ATTG ideal*
1	L	26.3	24.0	N	-11.0	-19.6	4.2	15.1	5.6	13.0	4.4
2	R	20.6	18.0	N	11.0	17.4	3.2	8.5	1.1	7.0	0.6
3	L	26.5	23.6	N	-14.0	-24.1	3.8	12.3	1.2	9.6	-0.5
4	L	30.8	19.0	N	-14.5	-24.9	4.2	15.5	3.3	4.5	-5.9
5	L	30.0	23.0	N	-8.2	-17.3	4.8	22.1	12.5	14.8	5.7
6	R	21.1	22.0	N	10.4	18.0	3.5	9.6	0.6	11.6	4.0
7	R	28.5	24.0	N	14.5	23.9	4.7	14.8	5.2	9.5	0.1
8	L	31.4	21.5	N	-10.6	-18.8	5.3	20.9	12.0	10.9	2.7
9	L	24.1	22.0	Y	0.4	-15.1	5.7	24.4	13.3	22.4	6.9
10	R	13.3	18.4	N	10.6	20.8	3.4	1.5	-9.7	7.8	-2.4
11	R	26.4	21.0	N	9.6	16.7	3.2	14.2	4.5	11.4	4.3
12	L	27.6	20.5	N	-11.1	-17.2	3.4	14.2	6.2	9.4	3.3
13	R	18.9	21.0	Y	7.1	14.7	3.1	10.6	1.0	13.9	6.3
14	L	27.6	26.1	N	-11.5	-20.5	4.3	16.2	6.3	14.6	5.6
15	L	48.4	25.5	N	-14.5	-27.9	7.3	37.0	24.0	10.9	-2.4
16	L	19.4	17.9	N	-8.5	-16.8	3.7	11.3	3.1	9.3	0.5
17	R	19.5	16.9	N	3.2	15.7	4.1	16.3	3.6	13.7	1.2
18	R	16.7	19.4	N	4.3	14.2	3.5	12.1	0.9	15.1	5.2
19	R	14.7	17.4	Y	-0.3	8.3	4.1	15.0	5.7	17.7	9.1
20	L	20.3	14.9	N	-1.5	-10.8	4.2	18.7	7.7	13.4	4.1
21	L	26.7	24.0	N	-10.5	-19.1	4.1	15.7	6.1	13.5	4.9
22	L	16.5	17.4	N	-5.4	-15.7	3.5	11.5	1.7	12.0	1.7

The possibility of mathematical determination of patellar ligament tibial insertion has a twofold interest. It should eliminate anterior peripatellar knee pain by accurately identifying the excessive lateral pressure syndrome well described clinically by P. Ficat,[5] and it should be useful to surgeons in avoiding excessive transpositions.

ACKNOWLEDGMENTS

In 1991, Miss Gaborit died in an avalanche. We hope the contribution her work and personal generosity made to this project is recognized not only here but in the hereafter.

REFERENCES

1. Basmajian JV, Harden TP, Regenos EM (1971) Integrated actions of the four heads of quadriceps femoris: An electromyographic study. Anat Rec 172:15–20.
2. Bernageau J, Goutallier D (1986) Mesure de la distance T.A.G.T. In Vigot (ed): Tomodensitometrie Corps Entier. Paris, Vigot, pp 512–514.
3. Castaing J, Burdin P (1977) Anatomie Fonctionnelle de l'Appareil Locomoteur: Le Genou. Paris: Vigot.
4. Caton J, Deschamps G, Chambat P, Lerat JL, Dejour H (1982) Les rotules basses—A propos de 128 observations. Rev Chir Orthop 68:317–325.
5. Ficat P (1973) Les desequililibres rotuliens. In: Les Déséquilibres Rotuliens. De l'Hyperpression a l'Arthrose. Paris: Masson.
6. Fujikawa K, Seedhom BB, Wright V (1983) Biomechanics of the patello-femoral joint. Part 1 a study of the contact and the congruity of the patello-femoral compartment and movement of the patella. Eng Med 12:3–11.
7. Garg A, Walker PS (1990) Prediction of total knee motion using a three-dimensional computer-graphic model. J Biomech 23:45–58.
8. Huberti HH, Hayes WC (1984) Patellofemoral contact pressures. The influence of Q-angle and tendofemoral contact. J Bone Joint Surg 66-A:715–724.
9. Huberti HH, Hayes WC, Stone JL, Shybut GT (1984) Force ratios in the quadriceps tendon and ligamentum patellae. J Orthop Res 2:49–54.
10. Insall J, Falvo KA, Wise DW (1976) Chondromalacia patellae. J Bone Joint Surg 58-A:1–8.
11. James SL (1979) Chondromalacia of the patella in the adolescent. In Kennedy JC (ed): The Injured Adolescent Knee. Baltimore: Williams and Wilkins, pp 205–251.
12 Julliard R, Friedrich P, Gabaudan P, Garna A (1979) Diagnostic radiographique de l'instabilité rotulienne—Les défilés en rotation externe. In: Premier Congrés de la Société Internationale de Genou. Lyon: Panneau scientifique.
13. Julliard R, Chalandre P, Friedrich P, Gabaudan P, Garna A (1982) Diagnostique radiographique de l'instabilité rotulienne. Les défilés en rotation externe. J Chir 119:169–175.
14. Julliard R, Cinquin P, Champleboux G, Gaborit L, Rose-Pitet L (1992) Mathematical determination of the ideal tibial insertion of the patellar tendon. In: IEEE Engineering in Medicine and Biology Society Proceedings, Paris, pp 1077–1078.
15. Lieb, Perry J (1968) Quadriceps function: An anatomical and mechanical study using amputated limbs. J Bone Joint Surg 50-A:1535–1538.
16. Lieb, Perry J (1971) Quadriceps function: An electromyographic study under isometric conditions. J Bone Joint Surg 53-A:749–758.
17. Maldague B, Malghem J (1987) Imagerie du genou en 1987. In: Cahier d'Enseignement de la SOFCOT. Conférence d'Enseignement, Expansion Scientifique Francaise, Paris, pp 343–370.
18. Maquet P (1981) Principe de biomecanique statique. Application au genou. In: Cahier d'Enseignement de la SOFCOT, Expansion Scientifique Francaise, pp 19–35.
19. Merchant AC, Mercer RL, Jacobsen RH, Cool CR (1974) Roentgenographic analysis of patello-femoral congruence. J Bone Joint Surg 56-A:1391–1396.
20. Seedhom BB, Takeda T, Tsubuku M, Wright V (1979) Mechanical factors and patellofemoral osteoarthrosis. Ann Rheum Dis 38:307–316.
21. Townsend PR, Rose RM, Radin EL, Roux P (1977) The biomechanics of the human patella and its implications for chondromalacia. J Biomech 10:403–407.